Three-Dimensional Simulation of HPCVD—Linking Continuum Transport and Reaction Kinetics with Topography Simulation

Wolfgang Pyka, *Student Member, IEEE*, Peter Fleischmann, Bernhard Haindl, and Siegfried Selberherr, *Fellow, IEEE*

***Abstract*— For wafer sizes in state-of-the-art semiconductor manufacturing ranging up to 300 mm, the uniformity of processes across the wafer becomes a very important issue. We present a fully three-dimensional model for the feature scale simulation of continuum transport and reaction determined high-pressure chemical vapor deposition processes suitable for the investigation of such nonuniformities. The newly developed three-dimensional approach combines topography simulation, meshing, and finite element method tools, and allows simulations over arbitrary geometries such as structures resulting from nonuniform underlying physical vapor deposition films. This enables the examination of film profile variations across the wafer for multistep processes consisting of low- and high-pressure parts such as Ti/TiN/W plug-fills. Additionally, the model allows a very flexible formulation of the involved gas chemistry and surface reactions and can easily be extended to process chemistries including gas phase reactions of precursors as observed in deposition of silicon dioxide from tetraethylorthosilicate (TEOS). We show simulation examples for a tungsten deposition process, which is applied as last step in a Ti/TiN/W plug-fill. For filling of an L-shaped trench, we show the transition from transport to reaction limited process conditions.**

***Index Terms*— High-pressure chemical vapor deposition (HPCVD), three-dimensional simulation, topography.**

I. Introduction

SIMULATION of etching and deposition processes assists in understanding the topography evolution in semiconductor device fabrication; it supports development and optimization of manufacturing equipment and process recipes. With the wafer size of today's semiconductor manufacturing ranging up to 300 mm, there is a considerable need for the control of the uniformity of processes for all dies on the wafer.

To some extent this problem can be tackled by placing more emphasis on equipment simulation which reveals trends in the general behavior of deposition rates, film thickness, film composition, and other characteristics of thin layers. Nevertheless, only feature scale simulation, preferably combined with a reactor scale equipment simulation, allows exact studies of film profiles differing due to flux, thermal, or other variations across the wafer.

In addition, the increasing complexity of devices and interconnect structures, which cannot be covered by expanding two-dimensional simulations with boundary conditions for infinitely long trenches or radially symmetric structures, requires a rigorous three-dimensional formulation of all involved physical and chemical phenomena.

In recent years a variety of three-dimensional simulators based on different approaches for the profile evolution has been presented. Most of them provide models for ballistic transport—also known as Knudsen transport—determined processes in the low-pressure regime.

SAMPLE-3D [1] includes macroscopic models for flux determined etching and deposition simulations based on a facet motion algorithm for the surface propagation. A similar segment-based approach [2] uses a redistribution model for reactive particles for simulating low-pressure chemical vapor deposition (LPCVD). In the level set methods developed at the University of California at Berkeley [3] and Stanford University [4], low-pressure processes are implemented by various combinations of analytic distribution functions for particle fluxes. Other two- or three-dimensional topography simulators working with similar macroscopic models are presented in [5] and [6].

A Monte Carlo approach of particle transport combines results from the three-dimensional reactor scale Monte Carlo particle transport simulator SIMSPUD with the feature scale simulator SIMBAD, thus resulting in interpolated three-dimensional deposition profiles [7]. This approach is very closely related to the manufacturing equipment since it incorporates experimental data such as target erosion profiles. Monte Carlo models combining particle transport simulation and surface reaction kinetics for plasma etching processes are also well established for multiple dimensions [8], [9]. All these simulators typically model processes at pressures below 1 torr. In this regime the Knudsen number as the ratio between gas mean free path and the characteristic feature length is well above one. Therefore the molecules inside the feature travel in line-of-sight and the particles undergo only very few collisions. Gas phase reactions mainly occur in the reactor space above the feature. Nonuniform film thickness is mainly caused by shadowing effects in the particle transport.

For pressures above 1 torr the gas mean free path becomes relatively small (Knudsen number $K_n \ll 1$) and the ratio between molecule–molecule and molecule–surface collisions increases drastically. Particle transport becomes determined by species effective diffusivities in the gas mixture. Two-dimensional simulations of such high-pressure CVD processes for low Knudsen number transport are reported in [10].

Manuscript received March 25, 1999; revised June 24, 1999. This paper was recommended by Associate Editor W. Schoenmaker.

The authors are with the Institut für Mikroelektronik, TU Wien, Wien A-1040 Austria.

Publisher Item Identifier S 0278-0070(99)09908-X.

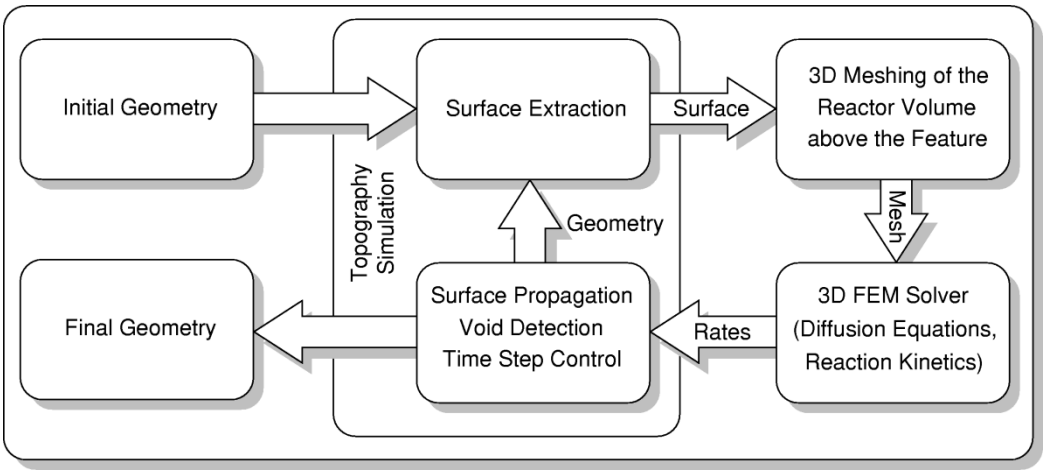

Fig. 1. Flow diagram for the CVD model.

The three-dimensional expansion of this simulator, EVOLVE-3D [11], combines the facet motion algorithm proposed by Scheckler [12] with the chemistry and reaction model of EVOLVE but only for the ballistic transport part.

To close this gap of missing high-pressure models in three-dimensional simulators, we have extended the two-dimensional continuum transport and reaction model and present a fully three-dimensional model for the feature scale simulation of arbitrary, multiple chemistry, high-pressure CVD processes in the continuum transport regime.

In [13], we have simulated ballistic transport determined sputter deposition of TiN by using analytical functions for the particle distributions. Simulations at arbitrary wafer positions were realized by setting the polar and azimuthal angle of the origin of the flux functions. Together with the newly developed high-pressure CVD model, all tools for an integrated process simulation including across wafer nonuniformities of ballistic transport and diffusion determined processes as suggested for two dimensions in [14] are now available.

The key issues for the model, which will be presented in detail in Section II, are surface propagation, meshing of the reactor domain above the feature, and diffusion and reaction simulation. Remarks on the integration of reactor and feature scale simulation will be given in Section II-F. Section III demonstrates a model for the deposition of tungsten, which is applied to a Ti/TiN/W plug-fill process and for various geometries and process conditions in Section IV.

II. Simulation Model

As indicated in Fig. 1, the high-pressure CVD (HPCVD) model consists of a combination of specialized tools, which are called iteratively by a control instance. After extracting the surface of the initial geometry, a three-dimensional mesh of the gas domain above the considered structure is generated. The differential equations describing the mass transfer and the reaction kinetics are set up and solved with a general finite element solver, which operates on the previously generated unstructured tetrahedral mesh. The resulting deposition rates are transferred to the topography simulator working with a cellular material representation, which performs the surface propagation leading to the new cellular topography. This procedure is repeated automatically for every time-step until the overall simulation time is completed. The parameters for the meshing tool and the description of the continuum transport model are set up in control files and remain unchanged during all time-steps. In this way, the process runs fully automatic without any further user interaction.

A. Surface Extraction

The first step in the simulation sequence is the preparation of the appropriate input for the meshing tool. The initial geometry is built up with a solid modeling tool based on the same cellular material representation as used for the deposition simulator. Therefore, the surface of the initial geometry as well as of the geometries resulting after each time-step has to be extracted in a triangular format, suitable as input for the meshing tool.

The conversion is accomplished with a marching cube algorithm [15]. It guarantees that all triangle points are in the center of the cell faces, which is necessary for an unambiguous correlation between triangle points and surface cells. The only exception are points touching the horizontal bounding box. In this case, the points are located at the edges of the cubes still permitting the unambiguous correlation. After the initial triangulation coplanar triangles are merged using a very small point to plane distance criterion according to [16]. In this way, a higher efficiency of the following meshing and finite element method (FEM) steps is achieved without loosing any topography information. An example of such a surface extraction can be seen in Fig. 2.

B. Meshing

The meshing tool described in detail in [17] uses a modified advancing front algorithm to generate a three-dimensional unstructured tetrahedral mesh. Starting with the initial surface given as a list of triangles, additional information such as the size of the reactor region above the feature and extra points within this region are necessary. The meshing tool allows the generation of point clouds in ortho or surface normal style. For the high-pressure CVD simulation, we achieved an adaptive

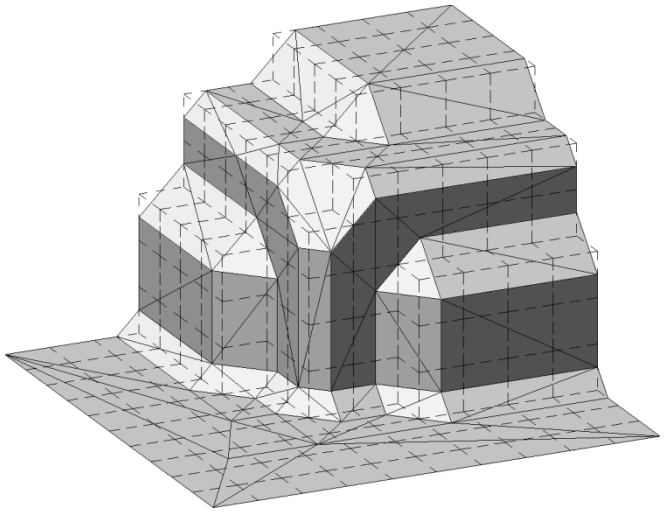

Fig. 2. Surface extraction from the cellular material representation (dashed lines) to a triangle description (shaded triangles in solid lines) using a marching cube algorithm and surface coarsening.

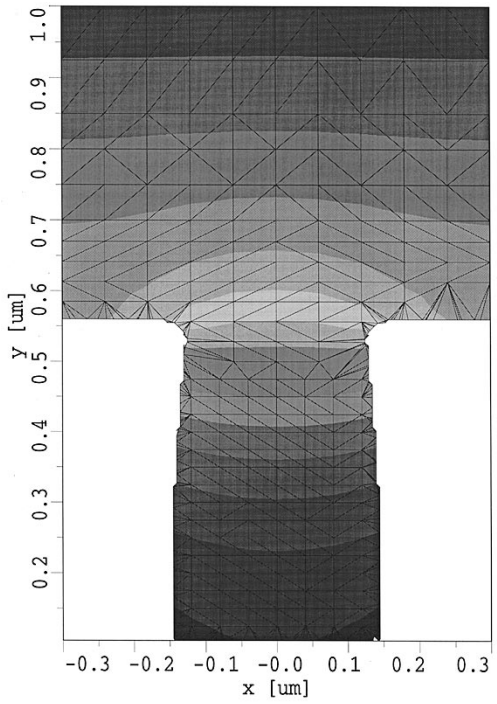

Fig. 3. Cross-section through the three-dimensional mesh showing the tetrahedra connecting adaptive ortho style point clouds in the interior with the boundary triangles generated by the surface extraction. Shading indicates the normalized WF_6 distribution.

resolution by specifying vertically stacked ortho style point clouds with different horizontal and vertical point distances. A cross-section of such a mesh can be seen in Fig. 3, a three-dimensional view thereof is depicted in Fig. 4(c). Note that Fig. 4(c) only reveals the triangular surface and the ortho style point cloud inserted above the wafer surface; it mostly omits the unstructured tetrahedra necessary to maintain the connectivity to the outer triangular surface.

When the surface has propagated after each time-step, it is possible that some of the initially defined points of the ortho style point clouds are "below" the new surface. Since the advancing front algorithm propagates from the initial surface in a well-defined direction, those points are never reached by the front and implicitly discarded. Therefore, it is possible to use one and the same control file and point clouds for meshing the structures of the different time-steps. This is a very important requirement for the automation of the simulation sequence.

C. Diffusion and Reaction Model

The chemistry model is set up with AMIGOS [18], an "analytical model interface and general object-oriented solver." The analytical model interface is an interpreter for translating mathematical expressions into a one-, two-, or three-dimensional discretized numerical representation. It provides an analytic input language for the formulation of the discretization scheme (finite elements, finite boxes) and of the considered partial differential equations. Since the differential equations are set up in an object-oriented formulation separately from the discretization scheme, the dimension of the model can be changed easily. Multiple volume and boundary models can be specified and assigned separately to different grids or boundaries. Afterwards, the global equation system is assembled according to the discretization scheme, and the global system matrix is passed on to the *general object-oriented solver*, a nonlinear numerical solver. The analytical model interface allows a great flexibility in choosing the involved gas species and chemical reactions.

For the presented formulation of the HPCVD model, which is derived from [10], we used a finite element discretization scheme. The governing principle for continuum transport determined CVD is species balance, i.e., time-dependent diffusion of gas species in the gas phase including homogeneous (volume) reactions

$$\frac{\partial c_i}{\partial t} = \nabla(D_i \nabla c_i) + R_j^{\mathrm{hom}} \tag{1}$$

and heterogeneous (surface) reactions

$$-D_i \frac{\partial c_i}{\partial n} = R_k^{\mathrm{het}} \tag{2}$$

with multiple species i, their concentrations c_i and their effective diffusivities D_i in the mixture. R_j and R_k represent the reaction rates of multiple chemical reactions j and k, which may occur either in the gas phase (hom) or at the wafer surface (het).

Moreover, we assume a constant concentration of the ith species at the top of the simulation domain

$$c_i = c_i^0 \tag{3}$$

and no flux across the side walls of the domain

$$\frac{\partial c_i}{\partial n} = n \nabla c_i = 0. \tag{4}$$

Equation (1) is formulated in an AMIGOS volume model assigned to the complete simulation domain. Equation (2) is set up in a boundary model description applied only to the wafer surface. Equations (3) and (4) are handled as Dirichlet boundary at the top of the simulation domain and

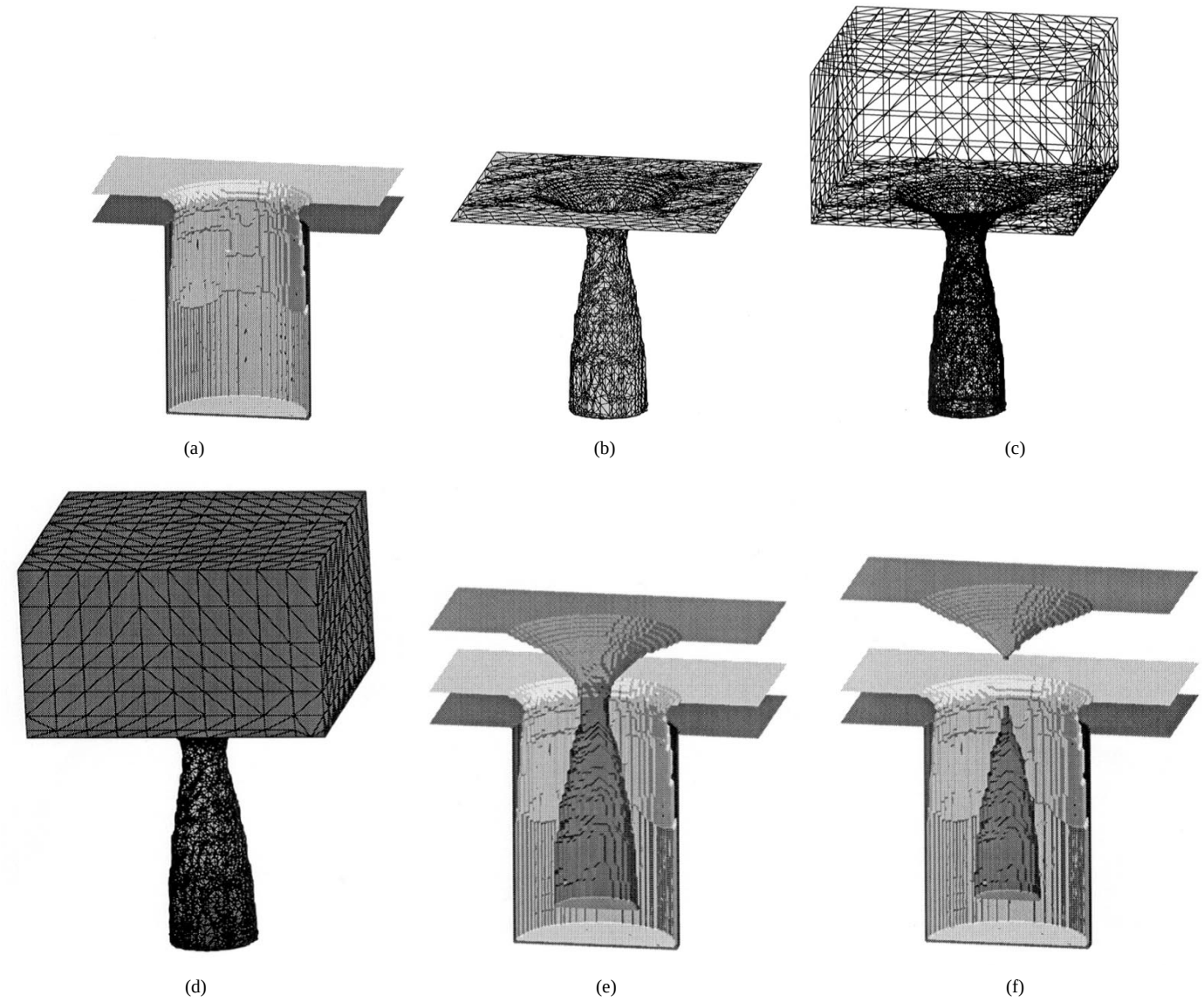

Fig. 4. Results of the single modules composing the overall HPCVD model: (a) shows the initial structure consisting of a circular via with a TiN PVD film, and (b)–(e) are results for (b) an intermediate time-step with extracted surface, (c) three-dimensional mesh, (d) distribution of WF_6 resulting from the continuum transport simulation, and (e) propagated surface; (f) shows the final geometry.

as Neumann condition at the domain sidewalls, respectively. The diffusion and reaction equations contain the concentrations of all involved gas species, which are coupled by the stoichiometry of the chemical reactions. Consequently, transport of gas molecules from the plasma above the wafer into the feature competes with surface reactions which transform the reactants to a solid material forming the deposited layer. This competition leads to a steady-state equilibrium and a geometry specific species concentration distribution depending on the ratio between gas diffusivities and surface reaction rates. For the steady-state, $\partial c_i/\partial t$ equals zero, and it is sufficient to solve the time-independent formulation of the diffusion equation

$$\nabla(D_i \nabla c_i) + R_j^{\text{hom}} = 0. \tag{5}$$

Putting the resulting steady-state concentrations at the boundary into the reaction rate equations leads to specific local deposition velocities, which are then passed on to the topography module.

D. Topography Simulation

For the surface propagation according to the deposition rates resulting from the previously described FEM calculations, we use a cell-based topography simulator, first presented in [19] with the extensions and improvements shown in [20]. The algorithm uses morphological operations derived from image processing. The geometry is represented by an array of cubic cells, which have a unique material index. A structuring element whose size depends on the local deposition rate is moved along the surface, and all vacuum cells hit by the element are switched to the index of the deposited material.

In contrast to the LPCVD model for the same simulator [13], the deposition rates for the high-pressure model are not calculated internally within the topography simulator but read from the AMIGOS result file. This file contains the triangles generated with the surface extraction from Section II-A and an additional rate value for each triangle point. The triangle

points positioned in the center of the cell faces are directly assigned to the corresponding surface cells. For maintaining a smooth and continuous surface evolution, it is necessary to apply structuring elements at all surface cells. This task is accomplished by a linear interpolation of the deposition rates within the triangles.

A very important task is the time-step control, especially when the process conditions lead to the formation of voids. In general, the CVD model uses a constant time-step for the surface propagation and the generation of a new mesh for taking into account the changed geometric conditions for the competition between diffusion and surface reaction. Depending on the interaction between diffusion velocity and reaction rates, a depletion of gas species at the bottom of the feature may be observed, which in consequence leads to strong variations of the local deposition rates, to the characteristic overhang structures, and to the formation of voids. Within the cellular material representation, a region of vacuum cells not connected with the gas domain above the surface can be detected easily and used for the control of void closure. To avoid the underestimation of the size of such a void by choosing a too-large time-step when the void is closed, the topography simulator checks for voids and reduces the time-step until it observes the first closure of the void when it detects the first formation of a void within the structure.

E. Process Control

In Fig. 4, the information that has to be transferred between the single modules (corresponding to the arrows in Fig. 1) is graphically summarized. The most important issue for an integrated simulation model is that *all* modules can be run fully automatically without any further user interaction. The crucial point hereby is the automation of the meshing tool, which could only be solved by using one and the same point cloud for all time-steps an the implicit elimination of outside points by the advancing front algorithm.

F. Integration with Reactor Scale Simulation

The presented model for CVD simulation works on feature scale and accounts for inhomogeneous gas concentrations due to gas depletion originating from the special geometric conditions within the feature and the competition between gas consumption at the surface and supply of reactants by diffusion. Boundary conditions, namely, the concentration of the gas species at the top of the simulation domain, are considered as constant and homogeneous within the dimension of the considered structure, which is up to a few micrometers.

This is, of course, not true when applying wafer scale to consider variations in heat distribution, gas flow, and gas depletion. In general, inhomogeneous thermal and flow conditions within the reactor lead to large variations in overall film thickness, film composition, profile evolution, and step coverage across the wafer. Basically, the CVD model could be formulated also in reactor scale. At this level, additional physical and chemical aspects have to be considered leading to a totally different set of differential equations, which has to be solved for the reactor geometry including the shape of the reactor chamber, wafer fixture, gas inlet and outlet, and gas flow conditions.

It is beyond the scope of our approach to cover also simulation and modeling on reactor scale, especially because reactor scale simulators dealing with different types of mass transport on nonmoving grids such as FLUENT[1] are commercially available. Nevertheless, our feature scale model allows the integration of results from equipment level simulations. Dirichlet boundaries at the top of the simulation domain can be set according to the concentration resulting from the equipment simulation. Together with the heat variations, they account also for changes in the species' effective diffusivities, thus changing the profile evolution by influencing the balance between diffusion velocity and reaction rate. Variations in growth rate and overall film thickness varying across the wafer can also be covered by adjusting the local deposition rate. By these means of integrating results from reactor scale simulation, our CVD model represents a link to the final prediction of the feature scale profile evolution in an integrated back-end process simulation.

The link between feature and reactor scale simulation is available for CVD as well as for ballistic transport determined processes. Beside the analytical functions used in [13] to simulate sputter deposition of TiN, it is also possible to include flux distributions resulting from three-dimensional Monte Carlo particle transport simulation as described in [7], accounting for experimentally measured target erosion profiles. The interfaces of our topography simulator to equipment simulation of low-pressure as well as of high-pressure processes allow fully integrated simulations of multiple step back-end processes such as Ti/TiN/W plug-fills, which will be described in Section IV-A.

III. HPCVD OF TUNGSTEN

The model for the deposition of tungsten was derived from the reduction of WF_6 with H_2

$$WF_6 + 3H_2 \rightarrow W + 6HF \tag{6}$$

forming HF as by-product. This reaction results in three diffusion equations for the gaseous species WF_6, H_2, and HF. Tungsten as reaction product is directly deposited as solid at the wafer surface and therefore has not to be considered for the diffusion. Of course the reaction chemistry is much more complicated with different adsorbed or chemisorbed intermediates and can be extended to a combined reduction with H_2 and SiH_4. For demonstration purposes, we will restrict ourself to an overall formulation of the chemistry even if more complex models can be formulated within the analytical model interface.

The derivation of effective species diffusivities in mixtures depending on composition, pressure, and temperature using the Chapman–Enskog equation and Lennard–Jones parameters σ and ϵ followed [10] and [21].

[1] [Online]. Available: HTTP: http://www.fluent.com/

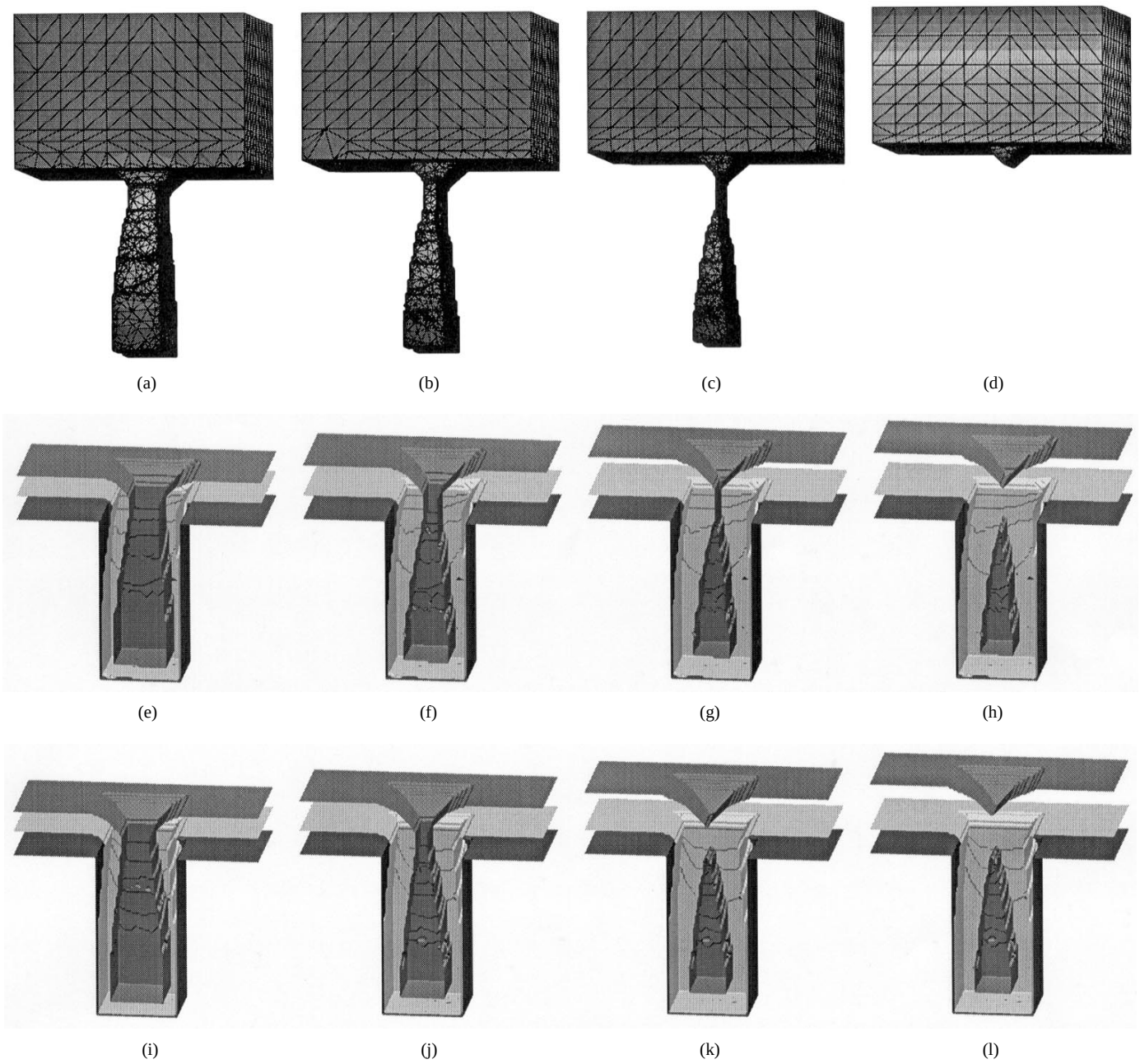

Fig. 5. Tungsten deposition in a rectangular via for different time-steps (from left to right). The topmost line depicts the volume meshes used for the diffusion simulation with the resulting WF_6 distributions; below are the corresponding film topographies for an off-center position. The bottommost line shows the symmetrical profile evolution for the same initial geometry at a center wafer position.

The deposition rate was experimentally found [22] to follow the expression

$$R_H = \frac{A \cdot \exp(-E_A/RT) \cdot [p(\mathrm{WF_6})] \cdot [p(\mathrm{H_2})]^{1/2}}{1 + B \cdot [p(\mathrm{WF_6})]}$$
$$A = 4.9 \times 10^{-2}\ \mathrm{mol \cdot torr^{-3/2} \cdot cm^{-2} \cdot s^{-1}}$$
$$B = 25\ \mathrm{torr^{-1}} \tag{7}$$

where A and B are experimentally determined constants, $p(\mathrm{H_2})$ and $p(\mathrm{WF_6})$ are hydrogen and WF_6 partial pressures, and E_A is the activation energy, which was set to 68.4 kJ/mol [14]. This rate expression is substituted into (2) and couples the concentrations of the three gaseous species by the stoichiometry of (6). When tungsten is formed at the wafer surface, a certain amount of WF_6 is consumed from the gas phase, thus reducing the concentration of WF_6. The same applies to the hydrogen concentration, differing only in the stoichiometric factor. Simultaneously, HF is formed and has to be added to the HF concentration in the gas phase.

IV. Results

In this section, we show results for the HPCVD of tungsten formed by the reduction of WF_6 with H_2. In Section IV-A, this process is used as final step in a Ti/TiN/W via plug-fill process. In this case, three-dimensional simulation is necessary for the investigation of film profiles varying with the wafer position.

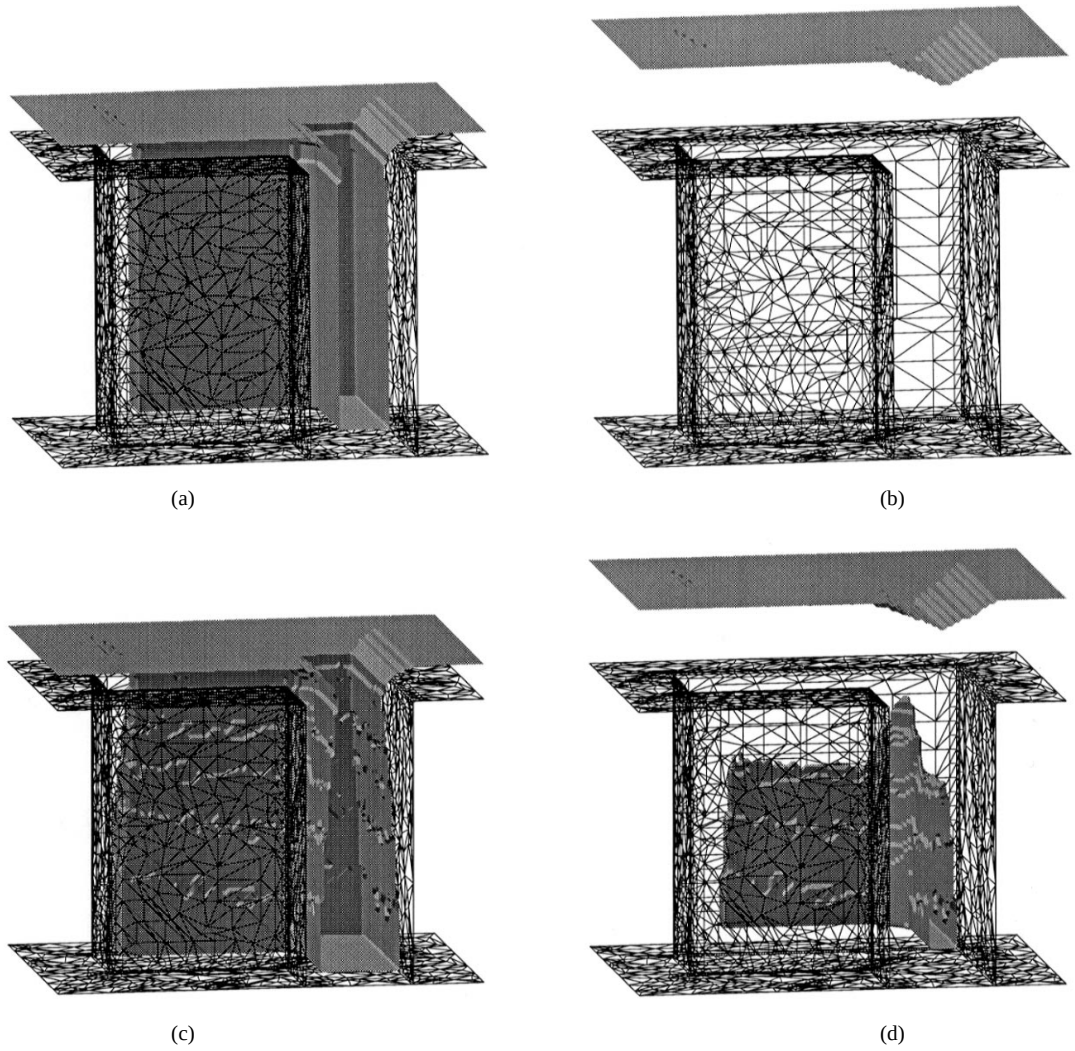

Fig. 6. Different process conditions for CVD of tungsten into an L-shaped trench. (a) and (b) represent an intermediate and the final profile for reaction limited process conditions, and (c) and (d) are analog time-steps for a diffusion limited process.

Last, Section IV-B demonstrates the transition between a diffusion and a reaction limited process for an L-shaped trench. Due to the geometry of the trench, this process also requires three-dimensional simulation.

A. Plug-Fill Process

We have applied CVD of tungsten at a pressure of 60 torr and a temperature of 703 K to an interconnect plug-fill process. A typical sequence for such a process consists of Ti PVD adhesion and TiN PVD barrier layers, a W nucleation CVD layer formed by silane reduction of WF_6 in presence of hydrogen, and a W bulk layer, deposited with hydrogen reduction of WF_6. Since we are interested in the final topography with special attention to the formation, size, shape, and location of voids, we neglect problems of adhesion of the films, which are usually addressed by the thin Ti and W nucleation layers and combine the four steps to a TiN PVD step followed by a W CVD step with hydrogen reduction of WF_6.

Fig. 4 shows the process sequence for a radially symmetric via at a position in the center of the wafer. For demonstration purposes, we artificially increased the reaction rate parameter to reveal the nonconformal films arising from the depletion of WF_6 within the feature due to the strong consumption of WF_6 at the feature surface. Fig. 4(a) depicts the TiN barrier layer over the initial geometry. According to the center wafer position exactly below the center of the sputter target, the distribution of particles arriving at the wafer surface is radially symmetrical resulting in a symmetrical TiN layer. In the following CVD step, with iterative surface extraction [Fig. 4(b)], mesh generation [Fig. 4(c)], and diffusion/reaction simulation [Fig. 4(d)] shown for an intermediate time-step this symmetry is maintained [Fig. 4(e)]. The final geometry for the cylindrical via with a diameter of 0.3 μm [Fig. 4(f)] contains a void whose top is significantly above the initial wafer surface approximately at the height of the TiN layer surface.

Fig. 5 illustrates the profile evolution for the same conditions but for a rectangular via at different positions on the wafer. Fig. 5(e)–(h) shows a sequence of time-steps for a peripheral wafer position. The corresponding volume meshes and WF_6 distributions are given above [Fig. 5(a)–(d)]. Fig. 5(i)–(l) denotes the center position for the same process parameters. In the case of the off-center position, the time-step from

Fig. 5(g)–(h) leads to the formation of a void. Since the fronts in Fig. 5(g) almost collide, the time-step control admits only a very small time-step leading to the closure of the void in Fig. 5(h). This can be observed in the smaller increase in the wafer surface layer thickness between Fig. 5(g) and (h) with respect to the increase between Fig. 5(f) and (g).

Due to the different geometric conditions, size and shape of the voids vary according to the underlying PVD layers. The profile of this layer depends not only on the initial geometry but also on the orientation of the structure with respect to the main particle flow in the sputter deposition. For the profiles of rectangular or elliptic vias, it is significant whether the main particle flux in the sputter deposition is parallel or perpendicular to the length axis of the via.

In the presented simulations, the variations in the void geometry originate from differing particle fluxes in the PVD step. The conditions for the W CVD layer are considered as homogeneous across the wafer. Thus the variations in the underlying PVD layer are continued throughout the CVD layer and underline the necessity of the rigorous three-dimensional approach for the CVD model.

Within the complete device manufacturing process, the topmost position of the void is of special interest. In the considered simulations, this position in the rectangular via (Fig. 5) is lower than in the circular via (Fig. 4) and even lower for the off-center position of the rectangular via. Additionally, the void formed at the off-center position is shifted off the center of the via.

B. L-Shaped Trench

The deposition of tungsten into an L-shaped trench with an aspect ratio of $1.5:4$ illustrates the ability of the model to account for a transition between reaction and transport limited process conditions. In the first example given in Fig. 6(a) and (b), the simulation is performed with the experimental parameters from (7). The reaction velocity at the wafer surface is very low; therefore, only a small fraction of WF_6 is extracted from the gas phase. The diffusion velocity is high enough that the consumed WF_6 is immediately replaced by the molecules coming from the plasma above the wafer. At all times, there is more WF_6 present than can be transformed by the surface reaction (6). Therefore, the film thickness is uniform over the whole structure, as can be seen in Fig. 6(a) for an intermediate time-step. Due to the larger width of the trench in the corner, it closes last, but no void is observed in the final structure Fig. 6(b).

A completely different situation is given in Fig. 6(c) and (d). Again, the reaction rate is increased in the same way as described in Section IV-A. The large reaction rate causes all WF_6 transported to the wafer surface to be immediately reduced to W. Diffusion from the reactor chamber is too slow and WF_6 in the feature becomes depleted, leading to a deposition rate decreasing downwards to the bottom of the feature. The resulting WF_6 depletion can be observed in Fig. 3. An intermediate time-step for the L-shaped trench given in Fig. 6(c) already shows the formation of an overhang profile. As can be observed in Fig. 6(d), this situation leads to the formation of a void, which closes last in the corner region of the trench with the top of the void almost reaching the initial wafer surface.

V. Conclusion

We have presented a three-dimensional model for the feature scale simulation of arbitrary, multiple chemistry, high-pressure CVD processes in the continuum transport regime. The rigorous three-dimensional approach has been realized by a combination of a cellular surface movement algorithm with an automated three-dimensional unstructured mesh generation and a three-dimensional FEM solver, allowing very flexible formulation of the involved differential equations and process chemistry. Simulations for different geometries at different wafer positions and for varying process conditions have revealed that special care has to be taken when large wafer sizes lead to nonuniformities of the film profiles. For processes with fast surface reactions leading to diffusion limited deposition conditions, the effect of overhang profiles leading to void formation is especially pronounced. Special emphasis has been put on the time-step control when the closure of voids is observed. Formation, size, shape, and especially the location of the top of the void are of special interest, when following process steps such as etching or chemical mechanical polishing may lead to opening of the vias, thus resulting in low quality or failure of the device.

Acknowledgment

The authors would like to acknowledge the valuable suggestions of V. Sukharev and discussions with H. Puchner and S. Aronowitz, all from LSI Logic Corp., Milpitas, CA. They would also like to acknowledge the support of the "Christian Doppler Forschungsgesellschaft," Wien, Austria, and Austria Mikrosysteme International AG, Unterpremstätten, Austria.

References

[1] E. W. Scheckler and A. R. Neureuther, "Models and algorithms for three-dimensional topography simulation with SAMPLE-3D," *IEEE Trans. Computer-Aided Design*, vol. 13, pp. 219–230, Feb. 1994.

[2] E. Bär and J. Lorenz, "3-D simulation of LPCVD using segment-based topography discretization," *IEEE Trans. Semiconduct. Manufact.*, vol. 9, pp. 67–73, Jan. 1996.

[3] J. A. Sethian and D. Adalsteinsson, "An overview of level set methods for etching, deposition, and lithography development," *IEEE Trans. Semiconduct. Manufact.*, vol. 10, pp. 167–184, Jan. 1997.

[4] Z.-K. Hsiau, E. C. Kan, J. P. McVittie, and R. W. Dutton, "Robust, stable, and accurate boundary movement for physical etching and deposition simulation," *IEEE Trans. Electron Devices*, vol. 44, pp. 1375–1385, Sept. 1997.

[5] M. Fujinaga and N. Kotani, "3-D topography simulator (3-D MULSS) based on a physical description of material topography," *IEEE Trans. Electron Devices*, vol. 44, pp. 226–238, Feb. 1997.

[6] S. Hamaguchi and S. M. Rossnagel, "Simulation of trench-filling profiles under ionized magnetron sputter metal deposition," *J. Vac. Sci. Technol. B*, vol. 13, no. 2, pp. 183–191, 1995.

[7] M. K. Sheergar, T. Smy, S. K. Dew, and M. J. Brett, "Simulation of three-dimensional refractory metal step coverage over contact cuts and vias," *J. Vac. Sci. Technol. B*, vol. 14, no. 4, pp. 2595–2602, 1996.

[8] J. P. Chang, A. P. Mahorowala, and H. H. Sawin, "Plasma-surface kinetics and feature profile evolution in chlorine etching of polysilicon," *J. Vac. Sci. Technol. A*, vol. 16, no. 1, pp. 217–224, 1998.

[9] R. J. Hoekstra and M. J. Kushner, "Comparison of two-dimensional and three-dimensional models for profile simulation of poly-Si etching of finite length trenches," *J. Vac. Sci. Technol. A*, vol. 16, no. 6, pp. 3274–3280, 1998.

[10] H. Liao and T. S. Cale, "Low-Knudsen-number transport and deposition," *J. Vac. Sci. Technol. A*, vol. 12, no. 4, pp. 1020–1026, 1994.
[11] ———, "Three-dimensional simulation of an isolation trench refill process," *Thin Solid Films*, vol. 236, pp. 352–358, 1993.
[12] E. W. Scheckler, "Algorithms for three-dimensional simulation of etching and deposition processes in integrated circuit fabrication", Ph.D. Dissertation, Univ. of California, Berkeley, 1991.
[13] W. Pyka and S. Selberherr, "Three-dimensional simulation of TiN magnetron sputter deposition," in *28th European Solid-State Device Research Conf.*, A. Touboul, Y. Danto, J.-P. Klein, and H. Grünbacher, Eds. Bordeaux, France: Editions Frontieres, 1998, pp. 324–327.
[14] V. Sukharev, K. Kumar, and E. J. McInerney, "An integrated simulation of across-wafer uniformity in Ti/TiN/W plug-fill," in *Proc. 15th Int. VLSI Multilevel Interconnection Conf.*, Santa Clara, CA, 1998, pp. 306–311.
[15] W. E. Lorensen and H. E. Cline, "Marching cubes: A high resolution 3D surface construction algorithm," *Comput. Graph.*, vol. 21, no. 4, pp. 163–169, 1987.
[16] W. J. Schroeder, J. A. Zarge, and W. E. Lorenson, "Decimation of triangle meshes," *Comput. Graph.*, vol. 26, no. 2, pp. 65–70, 1992.
[17] P. Fleischmann, W. Pyka, and S. Selberherr, "Mesh generation for application in technology CAD," *IEICE Trans. Electronics*, vol. E82-C, no. 6, pp. 937–947, 1999.
[18] M. Radi, E. Leitner, and S. Selberherr, "Amigos: Analytical model interface & general object-oriented solver," *IEEE J. Technol. Computer-Aided Design* [Online], vol. 18. Available: HTTP: http://www.ieee.org/products/online/journal/tcad/accepted/radi-feb99/
[19] E. Strasser and S. Selberherr, "Algorithms and models for cellular based topography simulation," *IEEE Trans. Computer-Aided Design*, vol. 14, pp. 1104–1114, Sept. 1995.
[20] W. Pyka, R. Martins, and S. Selberherr, "Efficient algorithms for three-dimensional etching and deposition simulation," in *Simulation of Semiconductor Processes and Devices*, K. De Meyer and S. Biesemans, Eds. Leuven, Belgium: Springer, 1998, pp. 16–19.
[21] E. J. Kim and W. N. Gill, "Modeling of CVD of silicon dioxide using TEOS and ozone in a single-wafer reactor," *J. Electrochem. Soc.*, vol. 141, no. 12, pp. 3462–3472, 1994.
[22] E. J. McInerney, T. W. Mountsier, and E. K. Broadbent, "A new analytic rate expression for hydrogen reduced tungsten," in *Conf. Proc. ULSI-VIII*, Materials Research Society, 1993, pp. 161–167.

Wolfgang Pyka (S'97) was born in Innsbruck, Austria, in 1970. He received the Dipl.-Ing. degree in materials science from the Montanuniversität Leoben in 1996. He is currently pursuing the doctoral degree from the Institut für Mikroelektronik, Technische Universität Wien, Austria.

In summer 1998 and 1999, he was a Visiting Researcher at LSI Logic, Milpitas, CA. His work is focused on simulation and modeling of etching and deposition processes and on algorithms for topographic simulations and three-dimensional geometry generation.

Peter Fleischmann was born in Kabul, Afghanistan, in 1969. He received the Dipl.-Ing. degree in electrical engineering from the Technische Universität (TU) Wien, Austria, in 1994. He is currently pursing the doctoral degree from the Institut für Mikroelektronik, TU Wien.

In December 1997 he was with NEC in Sagamihara, Japan. His research interests combine mesh generation with algorithms and data structures in computational geometry.

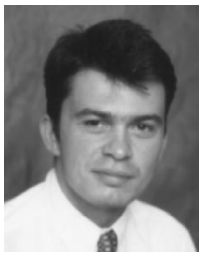

Bernhard Haindl was born in Wien, Austria, in 1969. He received the Dipl.-Ing. degree in communication and electrical engineering from the Technische Universität (TU) Wien, Austria, in 1995.

He worked for three years as a Software and Network Engineer in the area of air traffic control at Frequentis, Wien. He joined the Institut für Mikroelektronik, TU Wien, in 1998. His scientific interests include process and device simulation as well as software engineering.

Siegfried Selberherr (M'79–SM'84–F'93) was born in Klosterneuburg, Austria, in 1955. He received the Dipl.-Ing. degree in electrical engineering and the doctoral degree in technical sciences from the Technische Universität (TU) Wien, Austria, in 1978 and 1981, respectively.

He has been holding the *venia docendi* on computer-aided design since 1984. Since 1988, he has been the head of the Institut für Mikroelektronik, TU Wien, and since 1999 he has been Dean of the Fakultät für Elektrotechnik. His current topics of interest are modeling and simulation of problems for microelectronics engineering.